

This is an Open Access document downloaded from ORCA, Cardiff University's institutional repository: <https://orca.cardiff.ac.uk/id/eprint/163670/>

This is the author's version of a work that was submitted to / accepted for publication.

Citation for final published version:

Garg, Atul, Jangra, Parveen, Singhal, Dharendra, Pham, Thong M. and Ashish, Deepankar Kumar 2024. Durability studies on conventional concrete and slag-based geopolymer concrete in aggressive sulphate environment. *Energy, Ecology and Environment* 9 , pp. 314-330. 10.1007/s40974-023-00300-w

Publishers page: <http://dx.doi.org/10.1007/s40974-023-00300-w>

Please note:

Changes made as a result of publishing processes such as copy-editing, formatting and page numbers may not be reflected in this version. For the definitive version of this publication, please refer to the published source. You are advised to consult the publisher's version if you wish to cite this paper.

This version is being made available in accordance with publisher policies. See <http://orca.cf.ac.uk/policies.html> for usage policies. Copyright and moral rights for publications made available in ORCA are retained by the copyright holders.



# **Durability Studies on Conventional Concrete and Slag-Based Geopolymer Concrete in Aggressive Sulphate Environment**

by

**Atul Garg**

Assistant Professor, Department of Civil Engineering, DCRUST, Murthal, (Sonapat). Haryana,  
India.

Email: [atulgarg.civil@dcrustm.org](mailto:atulgarg.civil@dcrustm.org)

**Parveen** (Corresponding author)

Assistant Professor, Department of Civil Engineering, DCRUST, Murthal (Sonapat), Haryana

Email: [separveenjangra@dcrustm.org](mailto:separveenjangra@dcrustm.org)

**Dhirendra Singhal**

Retd. Professor, Department of Civil Engineering, DCRUST, Murthal (Sonapat). Haryana, India

Email: [dsinghald62@rediffmail.com](mailto:dsinghald62@rediffmail.com)

**Thong M. Pham**

UniSA STEM, University of South Australia, Mawson Lakes, SA, 5095, Australia.

Email: [thong.pham@unisa.edu.au](mailto:thong.pham@unisa.edu.au)

**Deepankar Kumar Ashish**

School of Engineering, Cardiff University, Cardiff CF24 3AA, UK Email:

[deepankar1303@gmail.com](mailto:deepankar1303@gmail.com)

# Durability Studies on Conventional Concrete and Slag-Based Geopolymer Concrete in Aggressive Sulphate Environment

Atul Garg<sup>1</sup>, Parveen<sup>1,\*</sup>, Dhirendra Singhal<sup>1</sup>, Thong M. Pham<sup>2</sup>, Deepankar Kumar Ashish<sup>3</sup>

<sup>1</sup>*Department of Civil Engineering, DCRUST Murthal-131039, Haryana, India.*

<sup>2</sup>*UniSA STEM, University of South Australia, Mawson Lakes, SA, 5095, Australia.*

<sup>3</sup>*School of Engineering, Cardiff University, Cardiff CF24 3AA, UK.*

## Abstract

As a potential substitute to conventional concrete, slag-based geopolymer concrete can be a promising material towards green and low carbon building approach. However, the lack of understanding of its performance subjected to sulphate environment can prohibit its use to some extent. This study examines the properties of conventional concrete exposed to a severe sulphate environment in comparison to slag-based geopolymer (SGPC). Plain cement concrete (PCC) also known as conventional concrete was cast using ordinary Portland Cement (OPC) as a binder. The durability of both types of concrete was examined by immersing test specimens in sulphate solutions (for varied salt concentrations of 2 and 4 g/l) for different curing ages up to a year. The performance of both types of concrete was studied for both mechanical and durability properties. Mechanical properties included compressive, tensile and flexural strengths (FS), while durability consisted of sorptivity, chloride diffusion, corrosion, EDS and SEM studies. The outcomes of this study revealed that the compressive (CS) and split tensile strengths (STS) of both OPC and SGPC decreased with the increase in magnesium sulphate salt concentrations and curing age. After being exposed to a 4% sulphate solution for 365 days, a decrease in the compressive strength was observed by 36.53% in SGPC and 55.97% in OPC, and a similar trend was found for the FS and STS. Rapid chloride permeability (RCPT) and sorptivity test results showed an increased diffusion with age and thus supported the findings of the compressive strength. Micro-structural properties were also studied, and observations showed that the formation of Sodium alumino-silicate hydrate (N-A-S-H) and Calcium alumino-silicate hydrate (C-A-S-H) was more obvious with the curing age in SGPC. At the same time, C-S-H gel formation decreased in conventional concrete with an increase in sulphate salt concentration. The cumulative effect of all these factors led to a much

29 higher corrosion rate of rebars embedded in conventional concrete than in SGPC. Therefore, slag-  
30 based geopolymer concrete performed better than conventional concrete in an aggressive sulphate  
31 environment for all curing periods.

32 **Keywords:** Slag-based geopolymer concrete (SGPC); Compressive strength; Tensile strength;  
33 Flexural strength; Chloride diffusion; Sorptivity; Polarization resistance.

34 **Abbreviations**

|                                       |         |
|---------------------------------------|---------|
| Calcium silicate hydrates:            | C-S-H   |
| Calcium alumino-silicate hydrate:     | C-A-S-H |
| Coarse Aggregate:                     | CA      |
| Compressive Strength:                 | CS      |
| Energy Dispersive Spectroscopy:       | EDS     |
| Fine Aggregate:                       | FA      |
| Flexural Strength:                    | FS      |
| Global warming potential              | GWP     |
| Ground granulated blast-furnace slag: | GGBFS   |
| Ordinary Portland Cement:             | OPC     |
| Rapid chloride permeability:          | RCPT    |
| Scanning electron microscopy:         | SEM     |
| Slag-based geopolymer concrete:       | SGPC    |
| Sodium alumino-silicate hydrate:      | N-A-S-H |
| Tensile Strength:                     | TS      |
| Ultrafine Slag:                       | UFS     |

35

## 361. Introduction

37 Concrete is the most extensively used construction material in the present scenario for rapid  
38 infrastructure development (Mustakim et al. 2021) as its demand approaches to 30 billion metric  
39 tons and it remains the main material used worldwide (Vázquez-Rowe et al. 2019). Concrete is  
40 often made from locally accessible resources such as cement, water, sand, and aggregates, with  
41 matrix cement serving as a binding agent (Edser 2005). Portland cement in conventional concrete  
42 used as binding material has several drawbacks. The production of traditional Portland cement  
43 (PC)-based concrete is energy-intensive (Malhotra 2010) and adds to greenhouse gas emissions by  
44 emitting roughly 5–7% of total CO<sub>2</sub> worldwide, which may climb by 50% in the future from  
45 current levels (Joseph et al. 2012). This fact shows that cement is not an environmentally-friendly  
46 material for long-term use because of its high energy consumption and CO<sub>2</sub> emission. Meanwhile,  
47 GBFS is advantage over conventional concrete as it has 44.70% lower global warming potential  
48 (GWP) (Barcelo et al. 2014; Robayo-Salazar et al. 2018). Clinker is created at temperature of  
49 approximately 1400<sup>0</sup>C, therefore, the energy required to achieve this temperature results for  
50 roughly 5% of worldwide CO<sub>2</sub> emissions (Malhotra 2010). Also, according to International Energy  
51 Agency, 0.81 kilogram of CO<sub>2</sub> produced for every kilogram of cement produced globally each  
52 year (Hendriks et al. 2003) which causes green- house affect. Further, durability of conventional  
53 concrete in an aggressive environment has been still questionable, and it has been a major concern  
54 of many standard guidelines to ensure concrete’s durability.

55 A new type of concrete coined geopolymers concrete has attracted a lot of interest from researchers  
56 as it utilizes waste materials such as fly-ash, ground-granulated blast-furnace slag (GGBFS), etc.  
57 and does not require much energy in its production (Pasupathy et al. 2021). Geopolymer materials  
58 are well known for having low embodied energy and low carbon emissions, and as a result, they  
59 are considered a viable substitute material for ordinary Portland cement (OPC) in conventional  
60 concrete. Previous studies also showed that a combination of rice husk and fly ash with OPC in a  
61 binder matrix, cured under a hot air curing (HAC) condition, gave the best compressive and  
62 flexural strengths with lower water absorption (Aljerf, 2015). The results reported in the recent  
63 past about its strength like compressive strength, flexural and split tensile strengths and durability  
64 properties under aggressive environments (Albitar et al. 2017; Jindal et al. 2018; Punurai et al.  
65 2018) are also encouraging.

66 The industrial waste product such as slag used to make geopolymer concrete primarily high in  
67 silica and alumina is activated by an alkali solution containing sodium/potassium (Mustakim et al.  
68 2021). In a previous study, it was discovered that the polymerization of geopolymer concrete was  
69 significantly influenced by alcofine (Parveen et al. 2018). Polymerisation is basically responsible  
70 for enhanced strength and dense microstructure. The study also showed that geopolymer concrete  
71 can obtain strength comparable to those of regular Portland and mixed-cement concrete even at  
72 room temperature. Muhammed et al. (2022) also studied the ultimate load of different types of  
73 reinforced concrete columns attacked by sulphate. Balamuralikrishnan and Saravanan (2021)  
74 studied the effect of addition of alcofine on the compressive strength and concluded that the  
75 addition of alcofine increases the strength. Thanh et al. (2022) studied the compressive strength of  
76 GPC using sea sand and sea water mixture and concluded that GPC concrete has a higher  
77 compressive strength than that of conventional concrete. Durability studies on geopolymer  
78 concrete exposed to aggressive environment also have been studied. Previously researcher also  
79 examined the performance of geopolymer concrete when exposed to acid solution (5% solution of  
80 acetic and sulfuric acid both) (Bakharev 2005b). It was observed that when GPC was prepared  
81 with sodium hydroxide and cured at elevated temperature, its performance was superior to  
82 conventional concrete in term of weight change, compressive strength and microstructural  
83 changes. When all the specimens were exposed to different sulphate environments (5% sodium  
84 sulphate and magnesium sulphate respectively and 2.5% sodium sulphate and 2.5% magnesium  
85 sulphate), the best performance was observed in geopolymer concrete. These specimens had 4-  
86 12% increase in strength when immersed into sulphate solution. The investigation period in these  
87 studies was, however, limited to short period of 9 months. It is still necessary to verify the  
88 material's long-term durability, particularly with regard to the protection of the reinforcing steel.  
89 Previous studies also indicated that sulphate environment or aggressive environment is more  
90 critical for durability prospective (Souza et al. 2020) and rendering rebars more susceptible to  
91 corrosion in case of conventional reinforced concrete. Therefore, this study has been undertaken  
92 to fill the gap and study the durability properties up to a period of one year in accelerated marine  
93 sulphate environment. Attempts have further been made to discuss the difference in mechanism in  
94 SGPC and conventional concrete.

95 The present study investigates the mechanical and durability properties of slag based geopolymer  
96 concrete (SGPC) and OPC concrete under an aggressive sulphate environment for one year. SGPC  
97 can be considered a sustainable material due to its low carbon emissions. This material can solve  
98 the environmental problems due to dumping of industrial wastes. Considering such issues and  
99 global demand of sustainable and durable products, this research intentionally introduces young  
100 researchers and industrialists an alternative product to conventional concrete. It is noted that  
101 geopolymer concrete has been developed in the field, there are numerous studies which explain  
102 the properties of GPC, but there is far more limited studies available in the literature which explore  
103 the performance of GPC in a aggressive environment for a long period. Furthermore, only basic  
104 data are available in public domain regarding strength and durability properties of SGPC in  
105 aggressive environments. This study, therefore, fills these research gaps.

## 106 **2. Materials and methods**

107 The properties of materials and methodologies used in this study are discussed below.

### 108 **2.1 Materials**

109 The chemical compositions of OPC and GGBFS (Ground granulated blast-furnace slag) are given  
110 in Table 1. Scanning electron microscopy (SEM) was used to determine the particle shapes of OPC  
111 and GGBFS, as shown in Fig 1.

112 **Table 1** Chemical composition of OPC and GGBFS (by weight).

| <b>Chemical composition</b> | CaO   | Al <sub>2</sub> O <sub>3</sub> | SiO <sub>2</sub> | Fe <sub>2</sub> O <sub>3</sub> | MgO  | K <sub>2</sub> O | Na <sub>2</sub> O | SO <sub>3</sub> | LOI  |
|-----------------------------|-------|--------------------------------|------------------|--------------------------------|------|------------------|-------------------|-----------------|------|
| OPC                         | 66.24 | 4.48                           | 18.02            | 4.31                           | 1.42 | 0.42             | 0.06              | 3.62            | 1.43 |
| GGBFS                       | 41.20 | 13.60                          | 38.70            | 2.0                            | 3.75 | ---              | 0.12              | 0.20            | 0.55 |

113

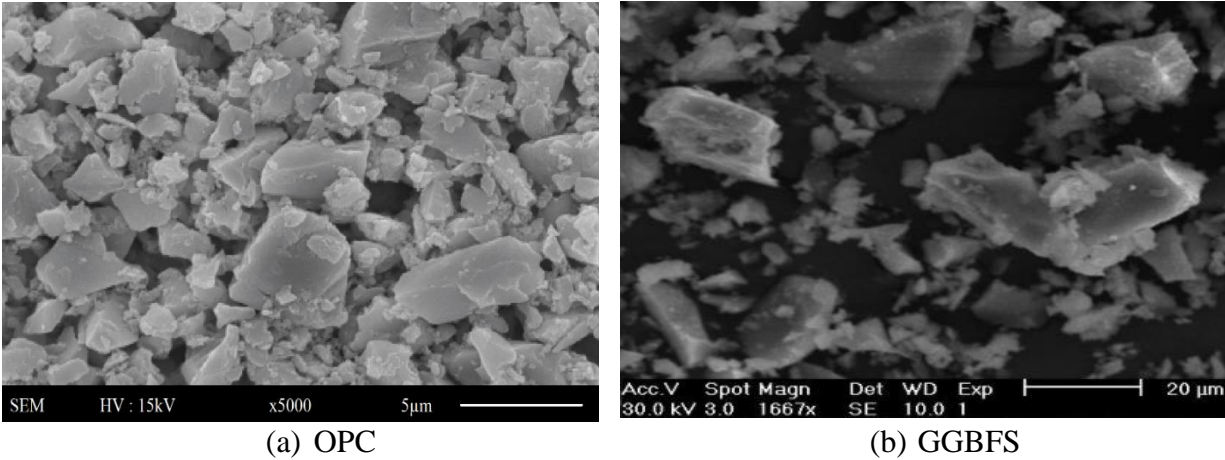


**Fig. 1** SEM images of OPC and GGBFS.

114 The coarse and fine aggregates complied with the requirements of IS 383 2016 (Bureau of Indian  
 115 Standards 2016). The specific gravity of coarse aggregates (CA) and fine aggregates (FA) was  
 116 tested and found to be 2.64 and 2.61, respectively. The coarse aggregates were of 14 mm mean  
 117 particle size.

## 118 **2.2 Sample preparation and testing**

119 In current study, specimens of OPC and SGPC were cast as cubes of 150 mm for the compression  
 120 tests, prism of 100 x 100 x 500 mm for flexural tests and cylinders of sizes 300 x 150 $\phi$  mm for  
 121 split tensile tests. For Rapid Chloride Permeability Test (RCPT) and sorptivity testing, cylinder  
 122 samples of sizes 100 x 50 $\phi$  mm and 70 x 30 $\phi$  mm were prepared, respectively. Also, for the  
 123 determination of polarization resistance, cube samples of 150 mm were cast with a steel rod at its  
 124 center and potential (mV) was measured for 200 s. To compare the mechanical and durability  
 125 properties, OPC and SGPC samples were cast for the target strength of 38.25 MPa, corresponding  
 126 to M30 grade as per IS:456 2000 (Plain and Reinforced Concrete - Code of Practice 2000). Clause  
 127 8.2.8 of IS:456 2000 (Plain and Reinforced Concrete - Code of Practice 2000) further suggests  
 128 minimum M30 grade concrete in a sea environment. The mix of OPC was designed following  
 129 IS:10262 2019 (Concrete mix Proportioning – Guidelines 2019), and Parveen and Singhal (2017)  
 130 proposed the mix design procedure and for GPC concrete. Accordingly, SGPC with the  
 131 activation's molarity M12 was designed with the help of available literature (Parveen et al. 2017).



132 For preparation of SGPC, ultrafine slag (UFS) named as alcofines was used as a binder. The mix  
 133 proportioning is summarized in Table 2 and a systemic testing flow chart is shown in Fig. 2.

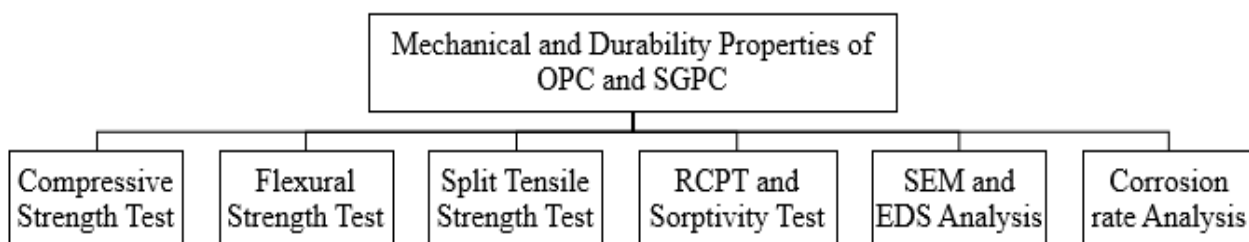
134 **Table 2** Mix design proportions used.

| Mix   | M1-OPC* | M2-SGPC* |
|---|---------|----------|
| OPC (kg/m <sup>3</sup> )                              | 365     | -        |
| GGBFS (kg/m <sup>3</sup> )                            | -       | 320      |
| Ultrafine slag (kg/m <sup>3</sup> )                   | -       | 80       |
| Sand (kg/m <sup>3</sup> )                             | 700     | 522      |
| Coarse Aggregate (kg/m <sup>3</sup> )                 | 1200    | 1240     |
| AAL/binder ratio                                      | -       | 0.45     |
| AAL (kg/m <sup>3</sup> )                              | -       | 180      |
| NaOH (kg/m <sup>3</sup> )                             | -       | 51       |
| Na <sub>2</sub> SiO <sub>3</sub> (kg/m <sup>3</sup> ) | -       | 129      |
| Na <sub>2</sub> SiO <sub>3</sub> /NaOH                | -       | 2.5      |
| Water (kg/m <sup>3</sup> )                            | 160     | 28       |
| Admixture (%)   | 1.5     | 1.5      |

135 Notes:

136 M1-OPC: Mix 1 with ordinary Portland cement

137 M2-SGPC: Mix 2 slag-based geopolymer concrete



138

139 **Fig. 2** Systemic testing flow chart.

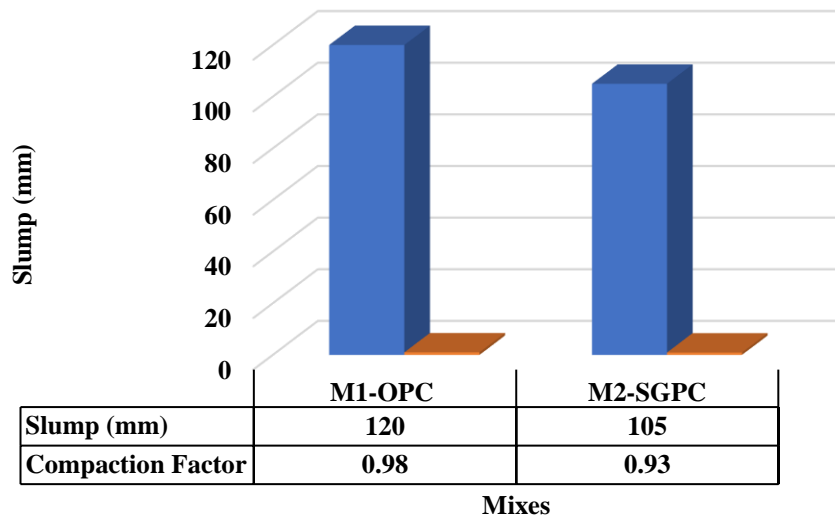
140 The specimens were cast and cured at room temperature, i.e.  $25\pm 3^{\circ}\text{C}$ . The specimens were filled  
141 in three layers, and compaction was done through a table vibrator. Specimens were taken out of  
142 the mold 24 hrs after the casting and then cured in water and in  $\text{MgSO}_4$  solutions containing 2 and  
143 4g/l salt, respectively.

144 To examine the performance of OPC and SGPC during the fresh stage, workability tests were  
145 performed by using slump and compaction factor tests. The compressive, flexural, and split tensile  
146 tests of OPC and SGPC were performed at ages 7, 28, 56, 90, 180, 270, and 365 days as per IS:  
147 516:2018 (Methods of Tests for Strength of Concrete 2018). The strength in all the discussions  
148 had been the average of five identical specimens. Rapid chloride permeability (RCPT) and  
149 sorptivity tests were also conducted at these curing ages as mentioned for compressive strength  
150 test except at 7 days. SEM and EDS studies and measurements of the corrosion rate were  
151 conducted at 180 and 365 days. For the durability study, the specimens were submerged in the  
152 solutions for half of the depth in order to expedite the corrosion process. A previous study  
153 suggested that the concentration of chloride salts in sea water varies from 3.96 to 23 g/l with an  
154 average of 19 g/l (Buenfeld et al. 1984). A previous study also showed that the concentration of  
155 sulphate salts in sea-water varies from 0.58 to 4 g/l with an average of 2 g/l (Liptak 1974).  
156 Accordingly, this study adopted the concentration of sulphate of 2 or 4 g/l. Therefore, submerging  
157 the specimens to half of the depth in solutions containing twice the average sulphate salt concretion  
158 of sea-water covered would simulate one of the critical condition of durability of climatic variation.

### 159 **3. Results and discussion**

#### 160 **3.1 Workability**

161 Fig. 3 shows the workability of the conventional concrete (M1-OPC), and slag-based geopolymer  
162 concrete (M2-SGPC) in terms of slump (mm) and compaction factor values.



163

164

**Fig. 3** Slump and Compaction factor of different concrete mixes.

165

166

167

168

169

170

171

172

The maximum slump (120 mm) and compaction factor (0.98) were observed in OPC, while SGPC showed a bit lower slump and compaction factor values (105 mm and 0.93, respectively). The viscosity of the alkaline solution used in SGPC may be the reason for the reduction in slump and compaction factors. Slump values more than 100 mm and compaction factor greater than 0.9 in SGPC indicated that GPC mixes are workable despite the fact that water content in GPC mixes was much less than OPC. Higher finer particles in GPC lead to lower workability as reported in a previous study (Patankar et al. 2013). Based on the workability test, it can be stated that both conventional and geopolymer concrete were workable as per Indian Standard guidelines.

173

### **3.2 Compressive strength**

174

175

176

In order to study mechanical properties, the compressive strength of both conventional and geopolymer concrete was determined at different ages as discussed above in both normal and aggressive environment.

177

#### **3.2.1 Compressive strength of water cured concrete samples**

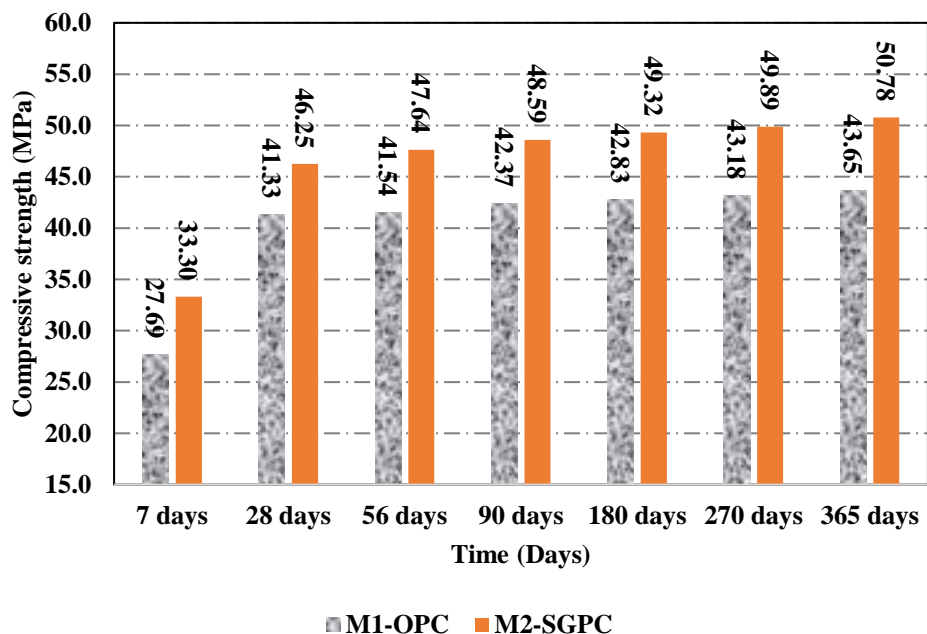
178

179

180

The compressive strength of both OPC and SGPC cured in water is shown in Fig. 4. It can be seen from the figure that the compressive strength increased with age, and the compressive strength of SGPC was higher than that of OPC. The compressive strength (46.25 MPa at 28 days) was

181 observed in M2-SGPC, while concrete with OPC (M1-OPC) showed a lower compressive strength  
 182 (41.33 MPa). The percentage increase in the compressive strength after 7 days was considerable  
 183 for both; however, it was no longer significant after 28 days. For example, M1-OPC and M2-SGPC  
 184 showed an increase of 49.25% and 38.88%, respectively, in the compressive strength at 28 days  
 185 when compared with those at 7 days. It can be also concluded from the figure below that SGPC  
 186 maintained higher strength throughout all the curing periods.



187

**Fig. 4** Compressive strength (CS) of water-cured concrete mixes.

### 188 3.2.2 Compressive strength of concrete exposed to MgSO<sub>4</sub> concentrations(2 and 4 g/l)

189 The effects of MgSO<sub>4</sub> concentrations (2 and 4 g/l) on the compressive strength of different mixes  
 190 were studied and have been shown in Fig. 5.

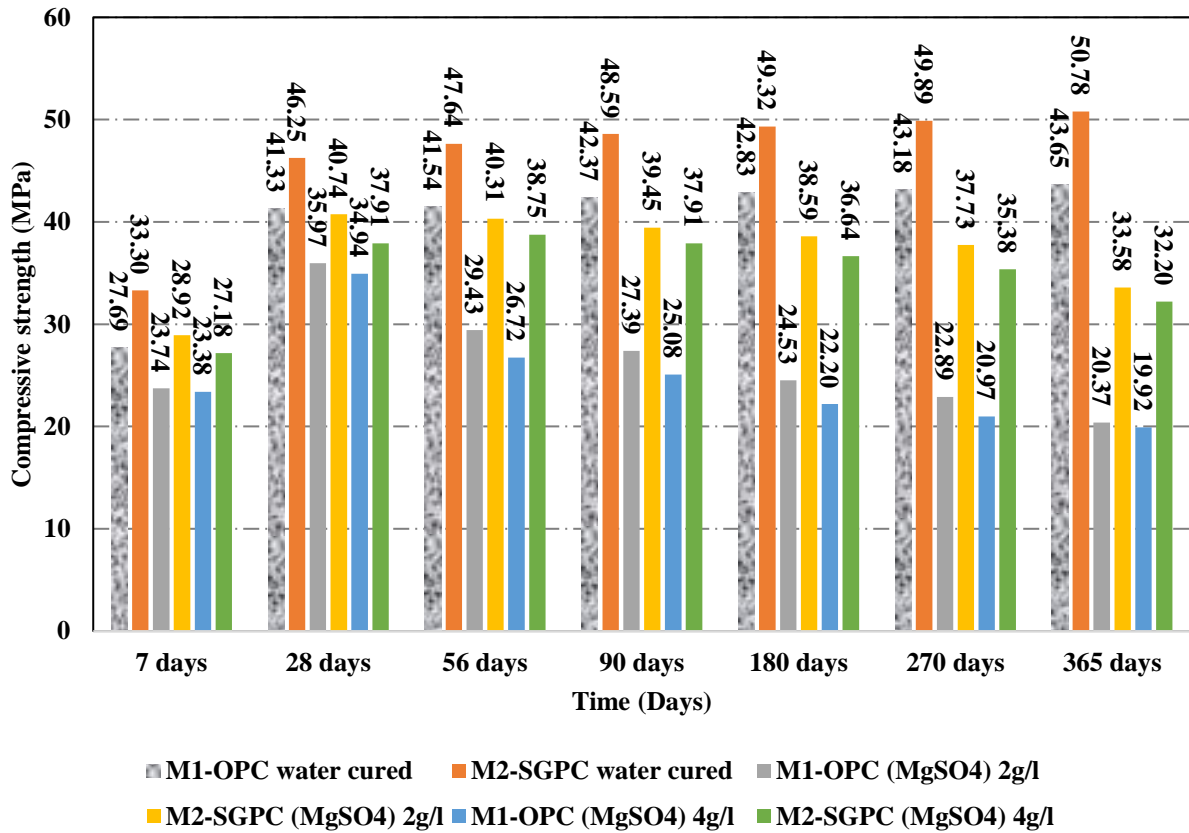


**Fig. 5** Compressive strength after exposure to a sulphate environment.

191 When samples were exposed to  $MgSO_4$  solution, a noticeable drop in the compressive strength  
 192 was observed for both the cases of OPC and SGPC after the curing age of 28 days with respect to  
 193 water cured specimens. During the curing phase, the compressive strength M1-OPC samples  
 194 decreased by a higher proportion than slag-based geopolymer concrete. Table 3 shows the  
 195 percentage decrease in the compressive strength of OPC and SGPC samples.

196 **Table 3** Percentage decrease of the compressive strength in sulphate environment.

| Mix | Curing period | Water cured sample compressive strength (MPa) | Compressive strength (MPa) of specimens exposed to $MgSO_4$ (2 g/l) | % decrease in Compressive strength (MPa) | Compressive strength (MPa) of specimens exposed to $MgSO_4$ (4 g/l) | % decrease in Compressive strength |
|-----|---------------|---|---|--|---|------------------------------------|
|     |               |   |   |  |   |                                    |

|         |          |       |       |       |       |       |
|---------|----------|-------|-------|-------|-------|-------|
| M1-OPC  | 28 Days  | 41.33 | 35.97 | 12.97 | 34.94 | 15.46 |
|         | 365 Days | 43.65 | 20.37 | 53.33 | 19.22 | 55.97 |
| M2-SGPC | 28 Days  | 46.25 | 40.74 | 11.91 | 37.91 | 18.03 |
|         | 365 Days | 50.78 | 33.58 | 33.81 | 32.2  | 36.53 |

197 The percentage drop in the compressive strength of M1-OPC was 55.97% after 365 days (in 4g/l  
198 solution) when compared with water cured samples, while M2-SGPC showed better performance  
199 (36.53% decrease in the compressive strength after 365 days at 4g/l) and this might be due to the  
200 formation of a considerably denser microstructure of SGPC in presence of alcofines (UFS), which  
201 is confirmed in the following SEM analysis.

### 202 **3.3 Flexural and split tensile strengths of concrete exposed to MgSO<sub>4</sub> concentrations (2** 203 **and 4 g/l)**

204 Figs. 6 (a) and 6 (b) show that the flexural and split tensile strengths follow the exact trend of the  
205 compressive strength results. A high MgSO<sub>4</sub> concentration, i.e. 4 g/l, resulted in a more significant  
206 strength drop for both M1-OPC and M2-SGPC when compared with the specimens cured in  
207 MgSO<sub>4</sub> concentration of 2 g/l. Similar results have also been reported by Bakharev (2005a). This  
208 observation suggests that an increase in sulphate salt concentration resulted in a decrease in the  
209 concrete strengths at all ages, irrespective of their binding materials.

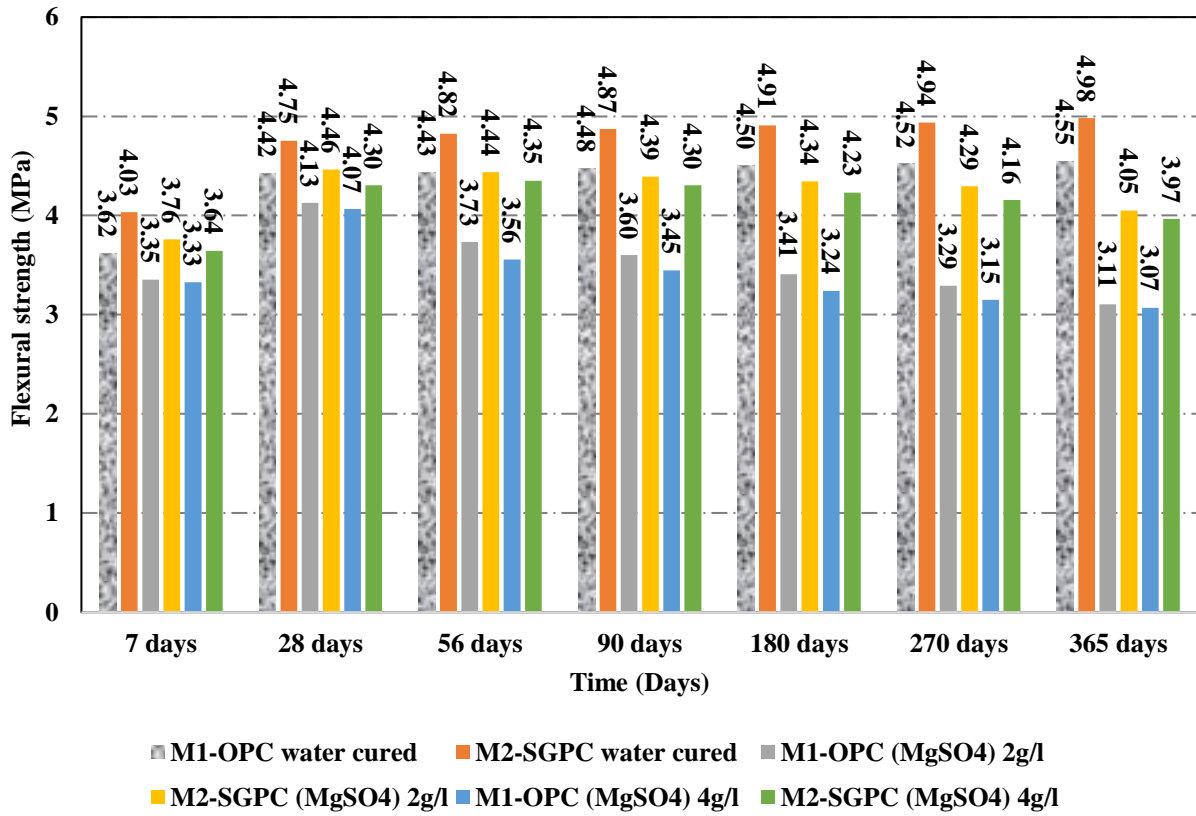


**Fig. 6(a)** Flexural strength of samples exposed to sulphate environment.

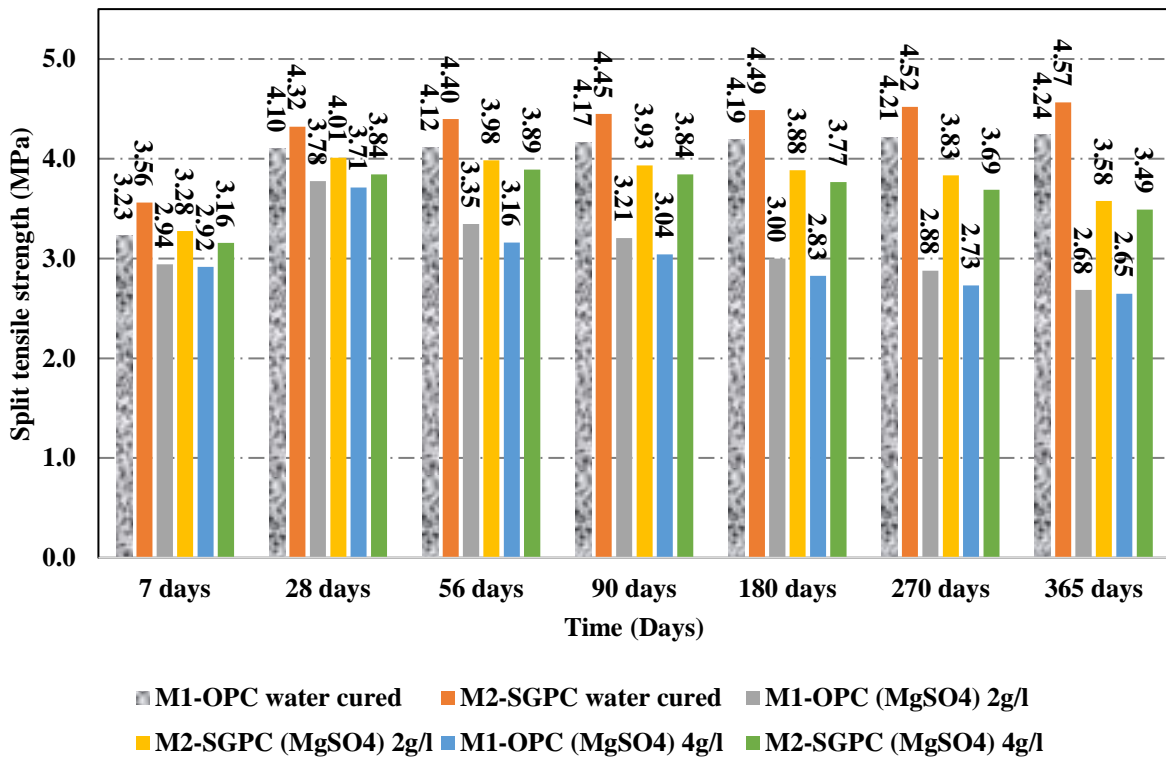


**Fig. 6(b)** Split tensile strength of samples exposed to sulphate environment.

210 The percentage drop in the flexural and split tensile strengths of M1-OPC samples when exposed  
 211 to MgSO<sub>4</sub> (4 g/l) was 32.52% and 37.50% as compared with water cured specimens at the same  
 212 age, respectively. Meanwhile, M2-SGPC submersed in the same sulphate solution showed a  
 213 20.28% and 25.26% drop in the flexural and split tensile strengths, respectively. It is obvious from  
 214 the observation above, M2-SGPC exhibited better structural performance in an aggressive sulphate  
 215 environment. This was attributed to the formation a much denser microstructure of SGPC in  
 216 presence of alcofines (UFS), which enhanced geopolymeric gel synthesis as also observed in the  
 217 previous study (Parveen et al. 2019).

### 218 3.4 Durability properties of slag based geopolymer (SGPC) and OPC

219 Durability investigations included RCPT tests, sorptivity, SEM and EDS studies, and polarization  
 220 resistance for the specimens cured under sulphate are presented in this section.

#### 221 3.4.1 Chloride penetration and sorptivity of water cured samples



222 The samples were exposed to an aggressive sulphate environment for examining their durability  
 223 characteristics. Furthermore, RCPT test was also conducted on these specimens cured in the  
 224 sulphate environment to study the permeability because durability of concrete significantly  
 225 depends on its permeability. The mechanism for chloride transportation are attributed to (a)  
 226 Diffusion (driven by concentration difference), (b) Permeation (driven by pressure difference) and  
 227 (c) Migration (driven by voltage difference). The average RCPT values over five specimens are  
 228 reported in Fig. 7(a). Furthermore, Fig. 7(b) presents the outcomes of sorptivity testing.

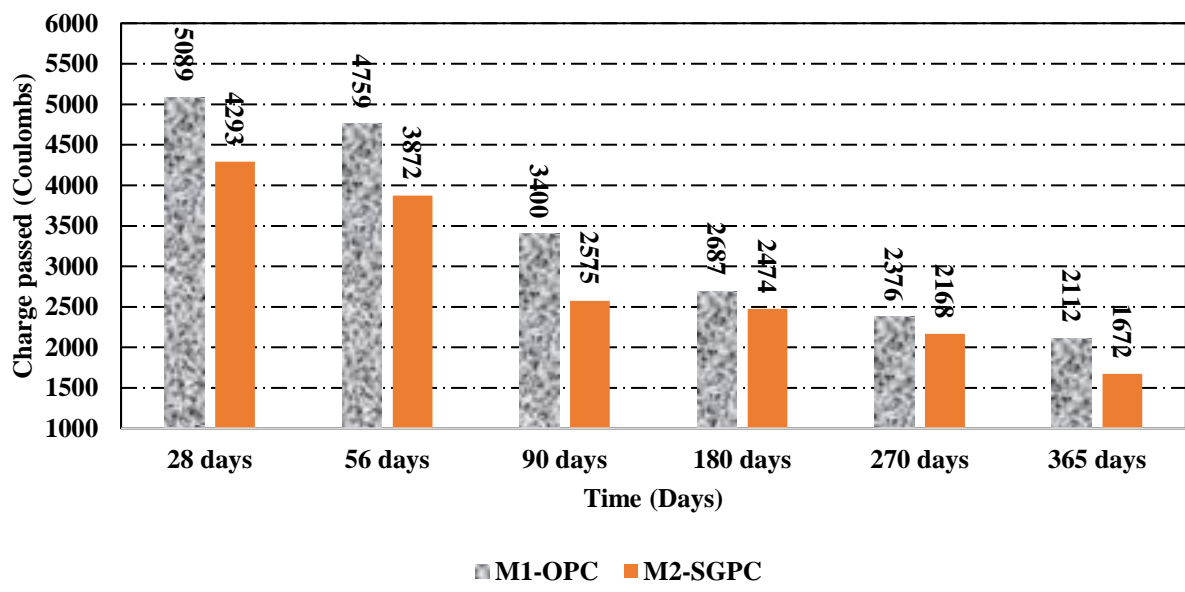


Fig. 7(a) RCPT values for the water cured concrete mixes.

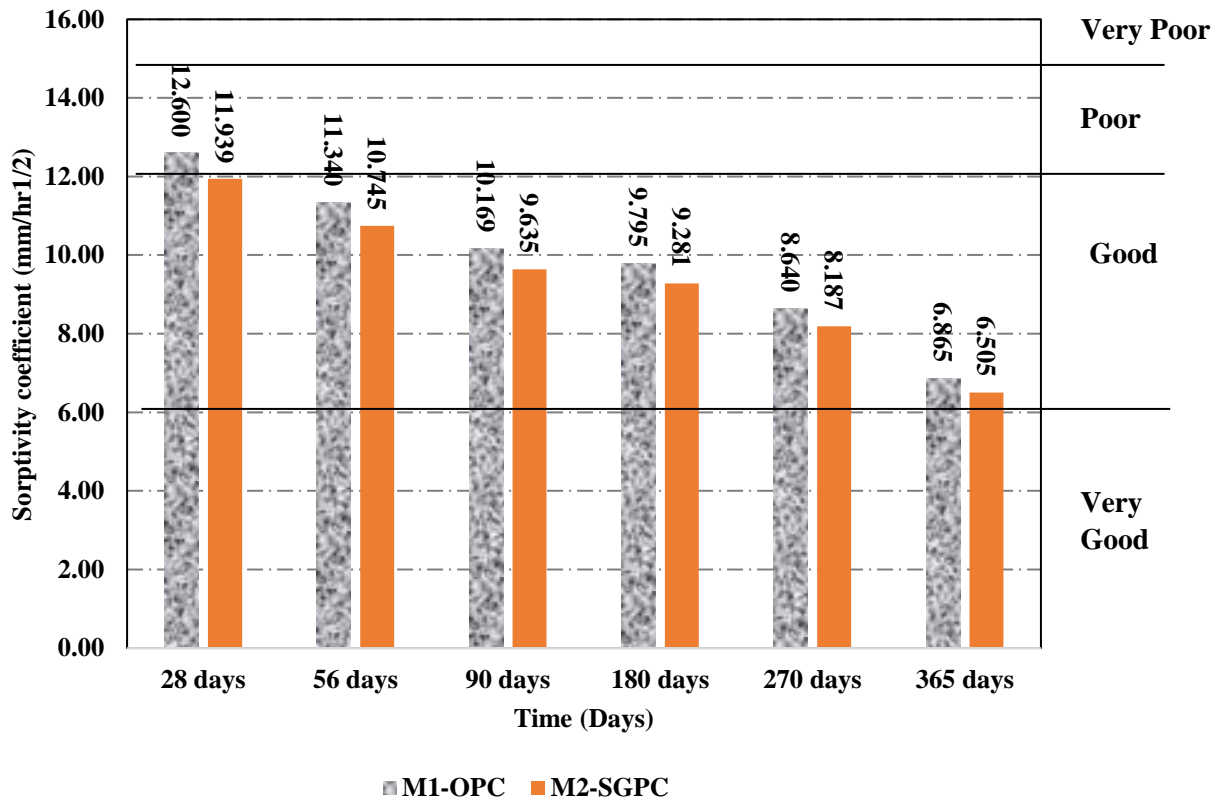


Fig. 7(b) Sorptivity coefficients for the water cured concrete mixes.

229 It is clear from the above figures that the charge passed in terms of coulombs and sorptivity  
 230 coefficients decreased with the increase in age in all the specimens. The decrease in charge passed  
 231 directly indicated that the permeability decreased with the increase in age. It is evident from these  
 232 figures that the permeability of M2-SGPC concrete was lower than M1-OPC at all ages, which  
 233 might again be due to better denser microstructure. The effects of adding nitrite- based inhibitor  
 234 in OPC was also studied by Sangoju et al. (2015) who concluded that with the addition of calcium  
 235 nitrite inhibitor there is reduction in the compressive strength of specimens. Also, there was an  
 236 increase in RCPT values when compared with the control samples. This may be due to the high  
 237 ionic nature of calcium nitrite inhibitor which causes more negative charges to pass through  
 238 concrete (Sangoju et al. 2015).

239 **3.4.2 Chloride penetration and sorptivity coefficient of concrete samples exposed to**  
 240 **MgSO<sub>4</sub> (2g/l and 4g/l)**

241 RCPT values were expected to increase when exposed to  $MgSO_4$  solution as the exposure of  
 242  $MgSO_4$  damages the cementitious properties as also observed in the previous study (Wee et al.  
 243 2000). The exposure of both M1-OPC and M2-SGPC in the sulphate environment increased the  
 244 chloride permeability with the curing age. This trend was just opposite when compared with their  
 245 respective specimens cured in water as shown in Fig. 8.

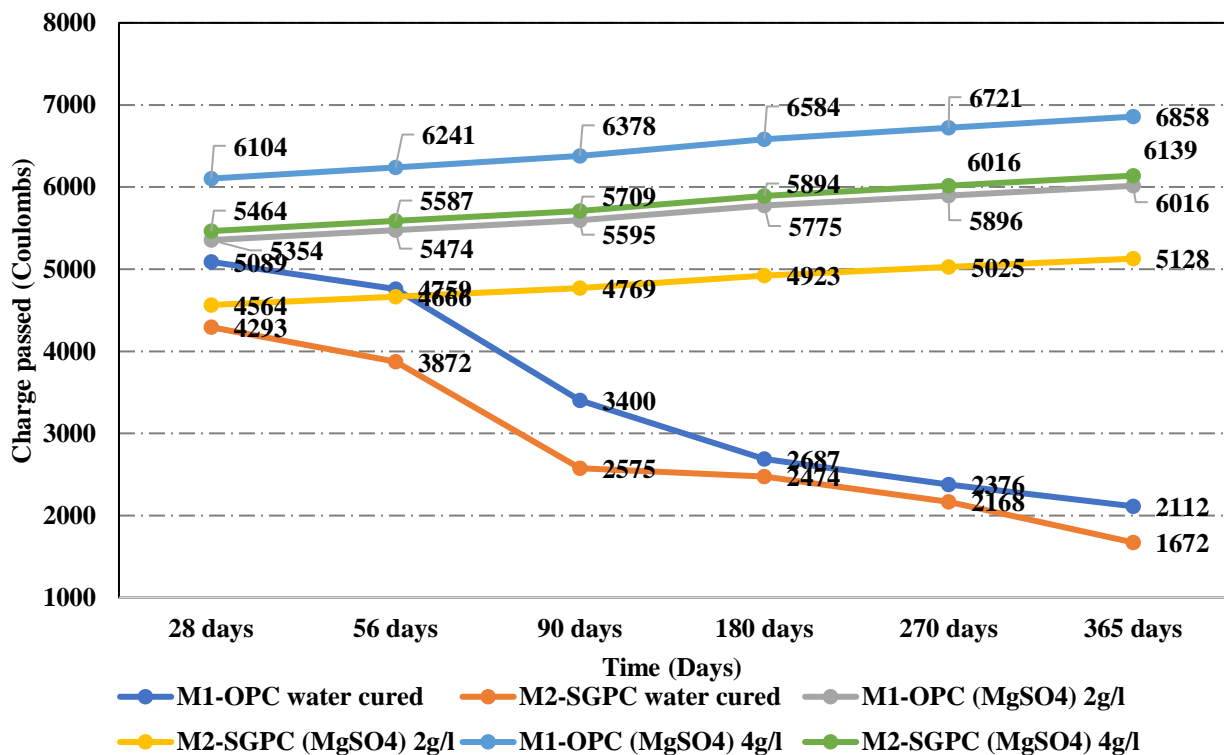


Fig. 8(a) RCPT values of different concrete mixes exposed to  $MgSO_4$  (2 g/l and 4 g/l).

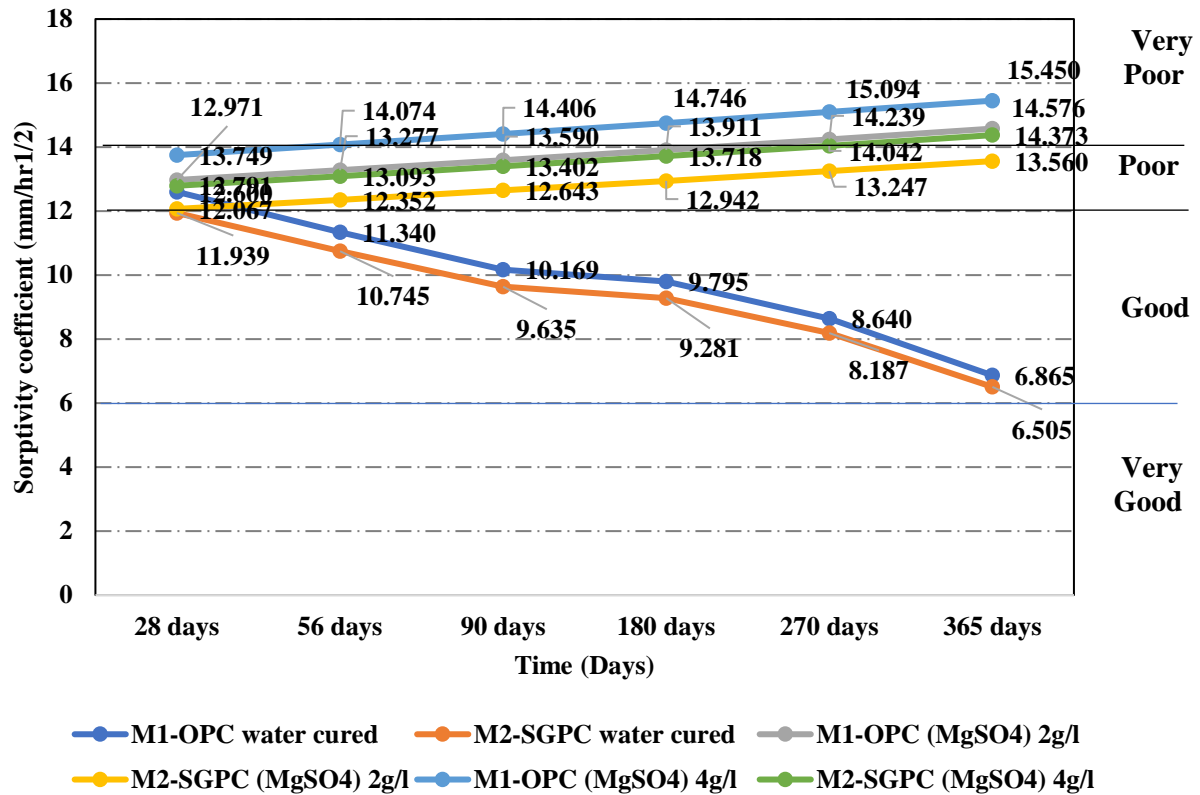


Fig. 8(b) Sorptivity coefficients of different concrete mixes exposed to MgSO<sub>4</sub> (2 g/l and 4 g/l)

246 The permeability increased with the concentration of MgSO<sub>4</sub> solution. For example, when mixes  
 247 of M1-OPC and M2-SGPC exposed to MgSO<sub>4</sub> (4 g/l) at 365 days are compared with the same  
 248 mixes exposed to MgSO<sub>4</sub> (2 g/l) at 180 days, RCPT results show 6,858 and 6,139 coulombs and  
 249 6,584 and 5,894 coulombs, respectively. These results confirmed that permeability was higher  
 250 when exposed to higher sulphate concentration. Fig. 8(a) further confirms that chloride  
 251 permeability of M2-SGPC specimens remained lower than M1-OPC specimens throughout the  
 252 curing period.

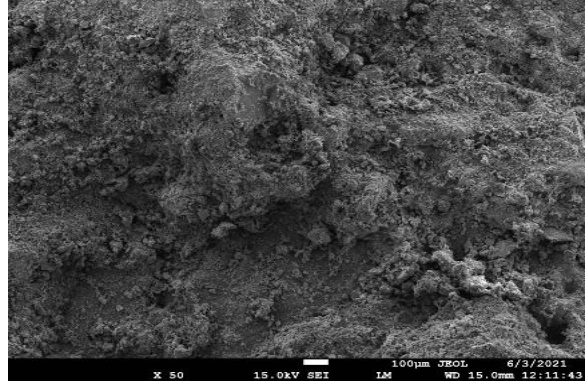
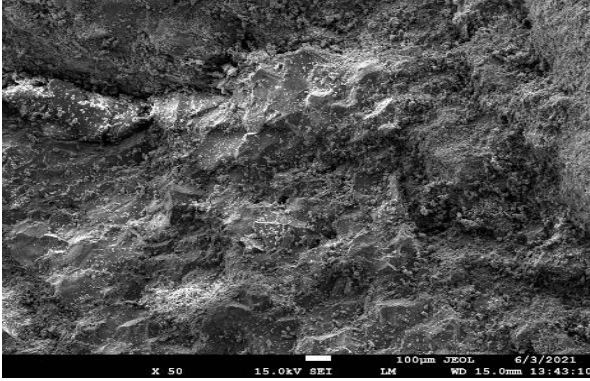
253 The same trend was observed in the sorptivity test. Sorptivity increased with the compressive  
 254 strength and RCPT test results as predicted. Exposure to higher MgSO<sub>4</sub> concentration, i.e., 4 g/l,  
 255 led to a substantial rise in sorptivity coefficients for both M1-OPC and M2-SGPC mixes, see Fig.  
 256 8(b). For example, when sorptivity of mixes M1-OPC and M2SGP exposed to MgSO<sub>4</sub> (4 g/l) at  
 257 365 days are compared with the same mixes exposed to MgSO<sub>4</sub> (2 g/l) at 28 days, it shows  
 258 sorptivity coefficients of 15.45, 14.37 and 12.97, 12.06, respectively. Fig 8(b) also confirms that

259 sorptivity coefficients were higher for the specimens exposed to higher  $MgSO_4$  salt concentration.  
260 The rise in sorptivity coefficients of geopolymer concrete specimens with  $MgSO_4$  exposure was  
261 lesser than that of OPC concrete specimens, making the SGPC more resistant to water permeation.  
262 A lower sorptivity of SGPC as compared to OPC has also been reported by Mathew and Usha  
263 (2016). The findings of the current study are also in line with the results reported by Gupta and  
264 Siddique (2020).

265 Above observations and discussions confirm that SGPC maintained better strength than OPC when  
266 exposed to sulphate environment at all curing periods. One of the reasons can be attributed to the  
267 less permeability of SGPC as compared to that of OPC as confirmed above with RCPT and  
268 sorptivity tests. Further, addition of alcofines in SGPC provided required strength even at room  
269 temperature, which was also reported by Saloni et al. (2020).

### 270 **3.5 SEM and EDS analysis**

271 Figs. 9 -14 show SEM images and EDS test results of OPC and SGPC. M1-OPC was cast with  
272 OPC containing  $C_3S$  and  $C_2S$ . These compounds, i.e.  $C_3S$  and  $C_2S$ , when hydrates form crystalline  
273  $Ca(OH)_2$ , floc, and hydrated calcium silicate gel before being subjected to a magnesium sulphate  
274 solution. During hydration of cement,  $C_3S$  and  $C_2S$  react with water and calcium silicate hydrate  
275 (C-S-H) is formed along with calcium hydroxide CH. This calcium silicate hydrates are the most  
276 important product for strength gain. It is the essence that determines the good properties of  
277 concrete. A heat increase happens due to the reaction between calcium silicate ( $C_3S$  and  $C_2S$ )  
278 which creates the silicate hydrate C-S-H. EDS study revealed that the main chemical product in  
279 the paste is C-S-H (calcium silicate hydrate) gel along with other products like NASH. Calcium  
280 silicate hydrate is indeed crucial component for extra strength gain in the geopolymer concrete.  
281 The maximum atomic percentage of silicon (Si) and calcium (Ca) were noticed.

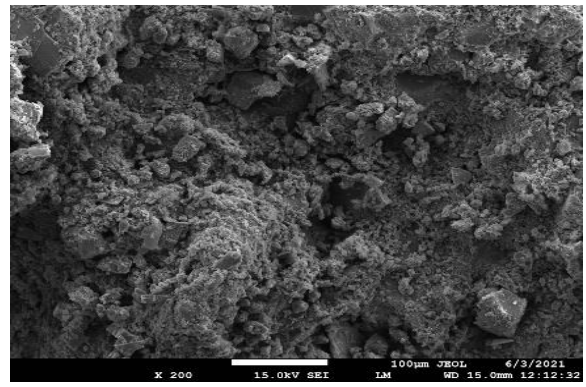
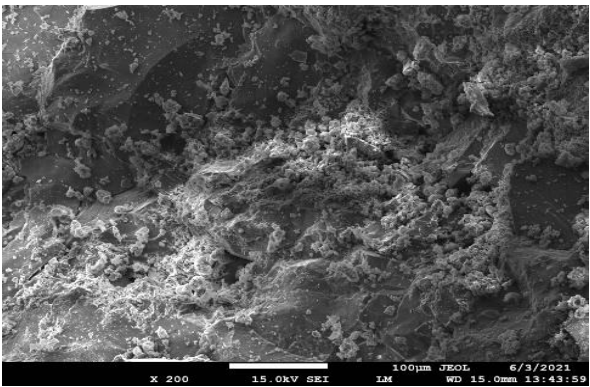


| Elements                   | O     | Al   | Mg   | Si   | S    | Ca    | Fe   | Na    | k    | Ca/Si | Si/Al |
|----------------------------|-------|------|------|------|------|-------|------|-------|------|-------|-------|
| <b>M1-OPC</b><br>Atomic %  | 58.95 | 1.28 | 0.84 | 9.75 | 1.82 | 25.79 | 1.57 | ----  | ---- | 2.65  | 7.62  |
| <b>M2-SGPC</b><br>Atomic % | 46.84 | 1.71 | 0.94 | 7.46 | 1.15 | 19.37 | 0.93 | 11.23 | 0.62 | 2.60  | 4.36  |

**Fig. 9(a)** Water cured OPC

**Fig. 9(b)** Water cured SGPC

**Fig. 9** SEM and EDS images of water cured concrete samples at 180 days

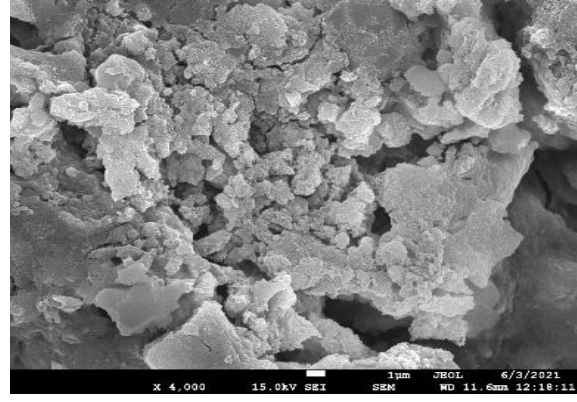
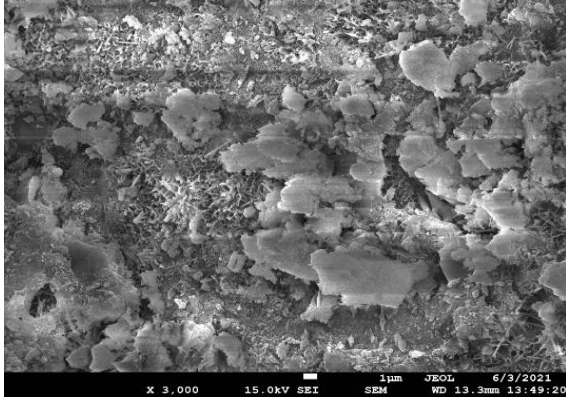


| Elements                   | O     | Al   | Mg   | Si   | S    | Ca    | Fe   | Na    | k    | Ca/Si | Si/Al |
|----------------------------|-------|------|------|------|------|-------|------|-------|------|-------|-------|
| <b>M1-OPC</b><br>Atomic %  | 57.04 | 1.15 | 0.89 | 9.81 | 1.83 | 28.01 | 1.27 | –     | –    | 2.86  | 8.53  |
| <b>M2-SGPC</b><br>Atomic % | 47.15 | 1.38 | 0.94 | 6.63 | 1.07 | 20.05 | 0.92 | 11.98 | 0.51 | 3.02  | 4.80  |

**Fig. 10(a)** Water-cured OPC

**Fig. 10(b)** Water-cured SGPC

**Fig. 10** EDS and SEM image of water cured concrete samples at 365 days

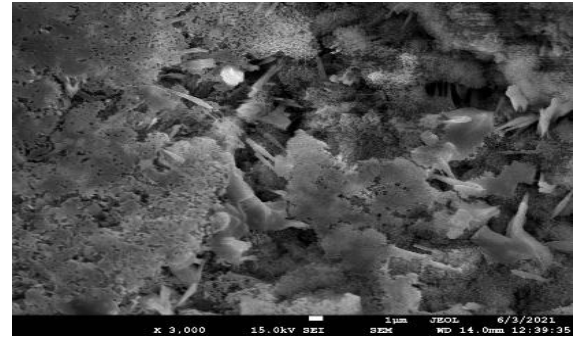
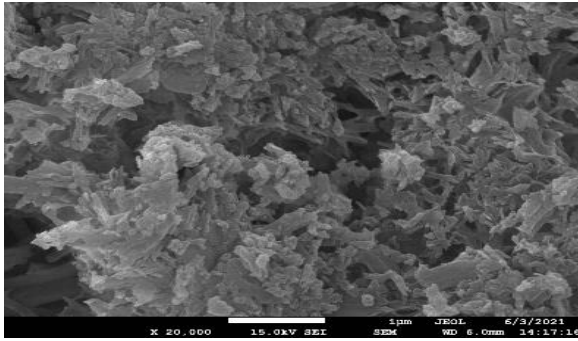


| Elements                | O     | Al   | Mg   | Si   | S    | Ca    | Fe   | Na    | k    | Ca/Si | Si/Al |
|-------------------------|-------|------|------|------|------|-------|------|-------|------|-------|-------|
| <b>M1-OPC Atomic %</b>  | 60.70 | 1.59 | 0.96 | 9.77 | 1.68 | 23.61 | 1.69 | ---   | ---  | 2.42  | 6.14  |
| <b>M2-SGPC Atomic %</b> | 51.34 | 1.76 | 1.1  | 7.32 | 1.25 | 14.76 | 0.95 | 10.03 | 0.62 | 2.02  | 4.16  |

**Fig. 11(a)** M1-OPC samples

**Fig. 11(b)** M2-SGPC samples

**Fig. 11** EDS /SEM images of samples immersed in  $MgSO_4$  (2g/l) solution for 180 days

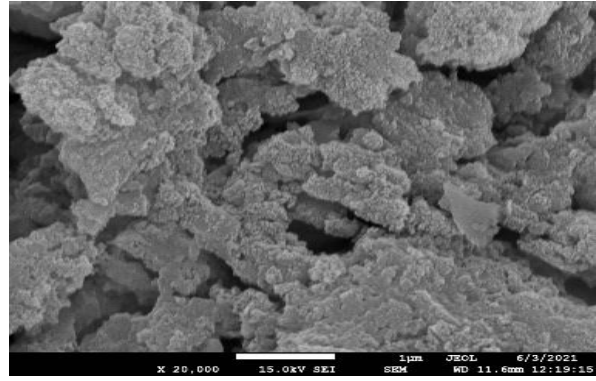
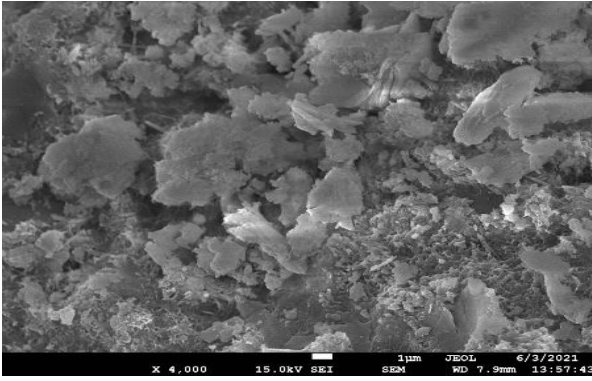


| Elements                | O     | Al   | Mg   | Si   | S    | Ca    | Fe   | Na   | k    | Ca/Si | Si/Al |
|-------------------------|-------|------|------|------|------|-------|------|------|------|-------|-------|
| <b>M1-OPC Atomic %</b>  | 61.20 | 1.61 | 0.89 | 9.59 | 1.94 | 23.01 | 1.76 | ---  | ---  | 2.40  | 5.96  |
| <b>M2-SGPC Atomic %</b> | 54.27 | 1.79 | 0.91 | 7.36 | 1.19 | 13.58 | 0.93 | 9.51 | 0.63 | 1.85  | 4.11  |

**Fig.12(a)** M1-OPC samples

**Fig.12(b)** M2-SGPC samples

**Fig. 12** EDS /SEM images of samples exposed to  $MgSO_4$  (4g/l) solution for 180 days



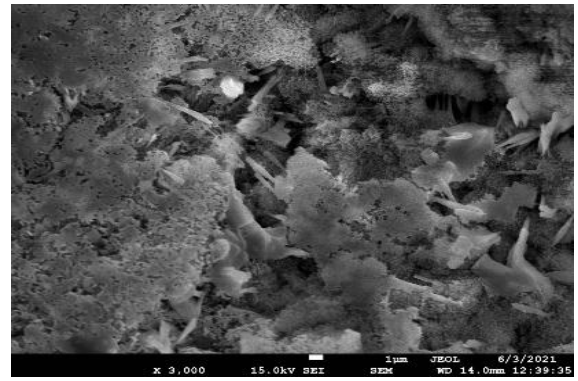
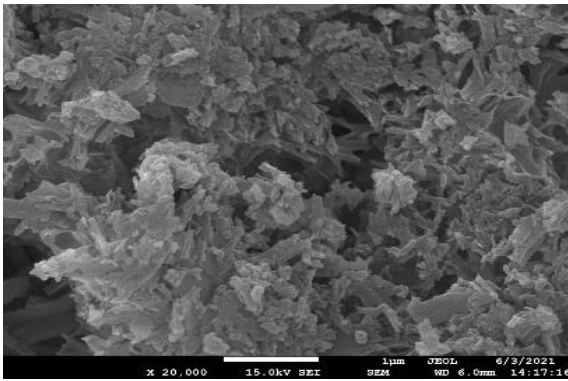
| Elements                | O     | Al   | Mg   | Si   | S    | Ca    | Fe   | Na   | k    | Ca/Si | Si/Al |
|-------------------------|-------|------|------|------|------|-------|------|------|------|-------|-------|
| <b>M1-OPC Atomic %</b>  | 61.22 | 1.20 | 1.23 | 9.63 | 1.93 | 22.93 | 1.86 | --   | --   | 2.38  | 8.03  |
| <b>M2-SGPC Atomic %</b> | 54.79 | 1.53 | 0.94 | 6.89 | 1.07 | 14.01 | 0.92 | 9.56 | 0.92 | 2.03  | 4.50  |

**Fig.13(a)** M1-OPC samples

**Fig. 13(b)** M2-SGPC samples

**Fig. 13** EDS /SEM images of samples exposed to MgSO<sub>4</sub> (2g/l) solution for 365 days

282



| Elements                | O     | Al   | Mg   | Si   | S    | Ca    | Fe   | Na   | k    | Ca/Si | Si/Al |
|-------------------------|-------|------|------|------|------|-------|------|------|------|-------|-------|
| <b>M1-OPC Atomic %</b>  | 63.06 | 1.23 | 0.96 | 9.8  | 1.68 | 21.3  | 1.97 | --   | --   | 2.17  | 7.97  |
| <b>M2-SGPC Atomic %</b> | 56.89 | 1.49 | 0.97 | 6.61 | 1.02 | 12.98 | 0.92 | 9.26 | 0.49 | 1.96  | 4.44  |

**Fig.14(a)** M1-OPC samples

**Fig.14(b)** M2-SGPC samples



**Fig. 14** EDS /SEM images of samples exposed to  $\text{MgSO}_4$  (4g/l) solution for 365 days

283 Figs. 9 and 10 show the SEM and EDS results of M1-OPC and M2-SGPC at 180 and 365 days  
284 when cured with water. A comparison of EDS results for OPC and SGPC specimens makes it clear  
285 that the total atomic percentage of Ca and Si in OPC were higher than that in SGPC. However, Na  
286 is the additional element found in SGPC; this confirms the formation of C-S-H gel in OPC and  
287 alkali-activated N-A-S-H in SGPC. Fig. 10 confirms that with an increase in age, Ca and Si  
288 contents increased in OPC, while in addition to Ca and Si contents alkali-activated N-A-S-H  
289 increased in SGPC. Although, it was quiet difficult to figure out the difference between the  
290 denseness of both the mixes but when we correlate SEM images (Fig. 10) with compressive  
291 strength results then it can be confirmed that SGPC was denser than OPC. This fact has further  
292 been supported by the RCPT and sorptivity results.

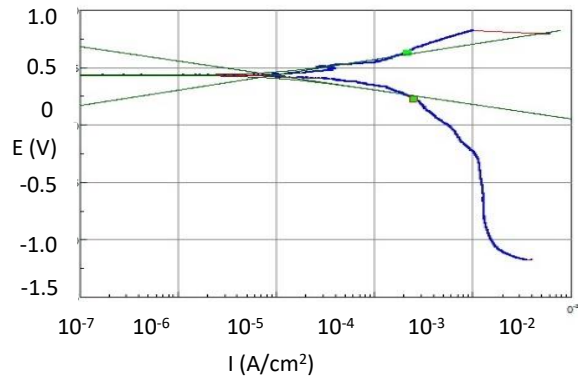
293 When comparing with water cured samples (Figs. 11 to 14), EDS results showed that with an  
294 increase in salt concentration  $\text{MgSO}_4$  (2g/l to 4g/l), the Ca/Si, and Si/Al ratio decreased at all ages.  
295 Also, the formation of C-A-S-H and N-A-S-H decreased in SGPC when specimens were exposed  
296 to sulphate salts, which explain the lower performance of SGPC when exposed to higher  
297 concentration of  $\text{MgSO}_4$  for a longer period.

298 Furthermore, Si/Al and Ca/Si atomic ratios were calculated to better understand the different  
299 binders and matrices. The above observations suggest that the compressive strength increased with  
300 Ca/Si and Si/Al ratios, particularly for water cured specimens. However, the compressive strength  
301 decreased when samples were exposed to the  $\text{MgSO}_4$  (2 g/l and 4 g/l) and SEM and EDS results  
302 confirmed this statement when showing decreased Ca/Si and Si/Al ratios. The above findings are  
303 in line of the tests results reported by other studies (Sasui et al. 2020). The results of the  
304 compressive strength are in well agreement with the EDS studies. High Ca/Si and Si/Al ratios  
305 boosted the development of calcium silicate-based compounds in the hybrid paste matrix, which  
306 mostly contributed to the increased strength (Saloni et al. 2021).

### 307 **3.6 Corrosion rate analysis of OPC and SGPC**

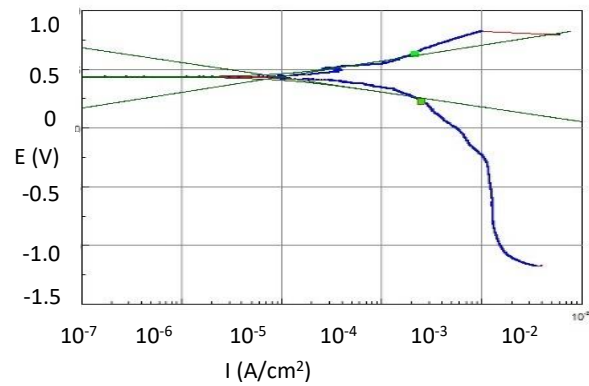
308 In order to study the corrosion rate of OPC and SGPC specimens exposed to sulphate environment,  
309 corrosion analysis was also conducted. The corrosion rate on steel bars embedded in concrete was

310 measured using Potentiostat. The corrosion results of the samples were measured after 180 and  
 311 365 days and are shown in Figs. 15 to 20.



Corrosion rate (mm/a) = 0.095

(a) Tafel plot of water cured conventional concrete at 180 days

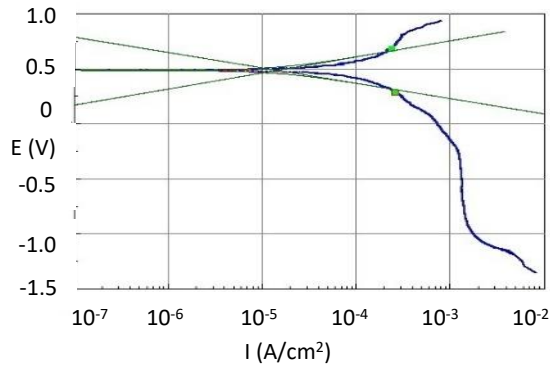


Corrosion rate (mm/a) = 0.082

(b) Tafel plot of water cured SGPC at 180 days

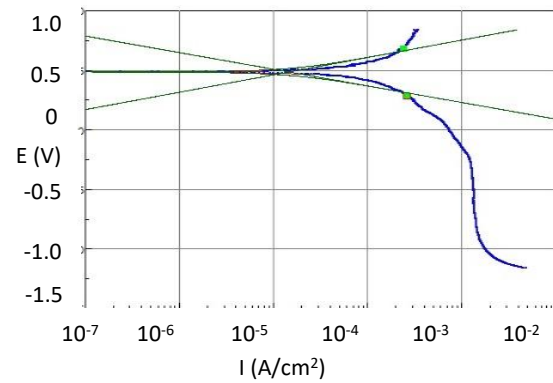
**Fig. 15** Tafel plot of OPC and SGPC under water curing at 180 days

312



Corrosion rate (mm/a) = 0.098

(a) Tafel plot of water cured conventional concrete at 365 days

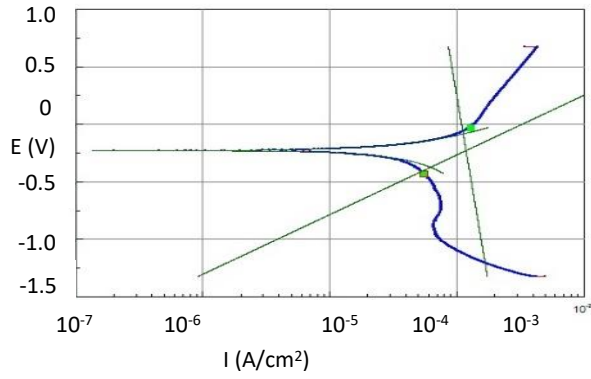


Corrosion rate (mm/a) = 0.087

(b) Tafel plot of water cured SGPC at 365 days

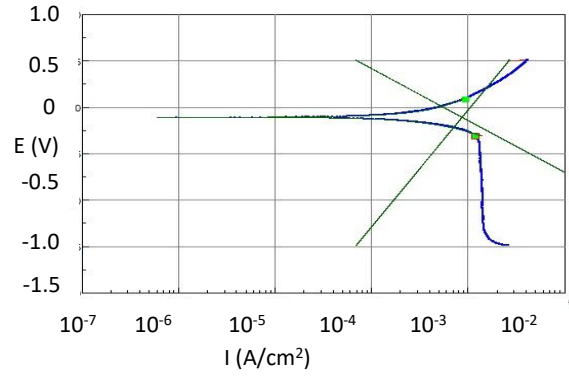
**Fig. 16** Tafel plot of OPC and SGPC under water curing at 365 days

313



Corrosion rate (mm/a) = 0.615

(a) Tafel plot of M1-OPC concrete sample exposed to  $\text{MgSO}_4$  (2 g/l) at 180 days

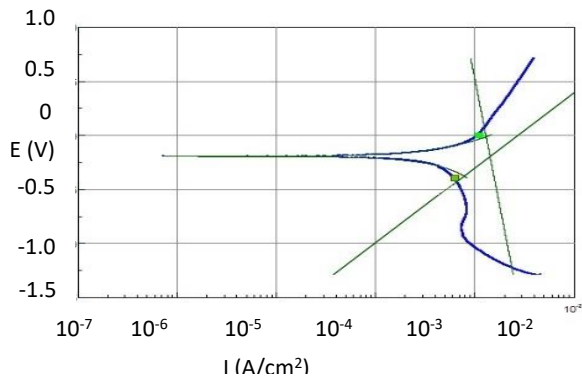


Corrosion rate (mm/a) = 0.569

(b) Tafel plot of M2-SGPC concrete sample exposed to  $\text{MgSO}_4$  (2 g/l) at 180 days

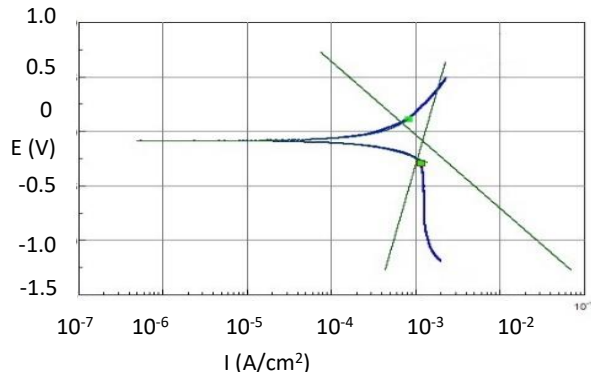
**Fig. 17** Tafel plot of OPC and SGPC under sulphate environment (2 g/l) at 180 days

314



Corrosion rate (mm/a) = 0.675

(a) Tafel plot of M1-OPC concrete sample exposed to  $\text{MgSO}_4$  (2 g/l) at 365 days



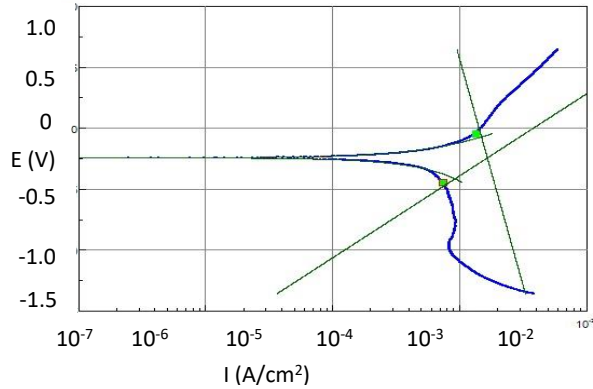
Corrosion rate (mm/a) = 0.598

(b) Tafel plot of M2-SGPC concrete sample exposed to  $\text{MgSO}_4$  (2 g/l) at 365 days

**Fig. 18** Tafel plot of OPC and SGPC under sulphate environment (2 g/l) at 365 days

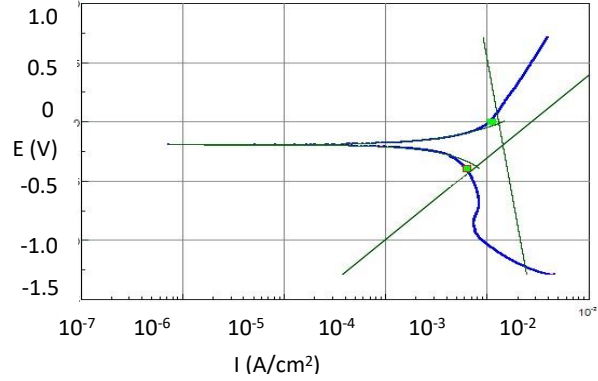
315

316



Corrosion rate (mm/a) = 0.628

(a) Tafel plot of M1-OPC concrete sample exposed to  $\text{MgSO}_4$  (4 g/l) at 180 days

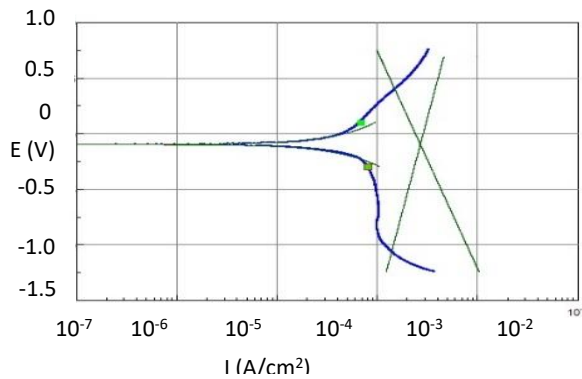


Corrosion rate (mm/a) = 0.608

(b) Tafel plot of M2-SGPC concrete sample exposed to  $\text{MgSO}_4$  (4 g/l) at 180 days

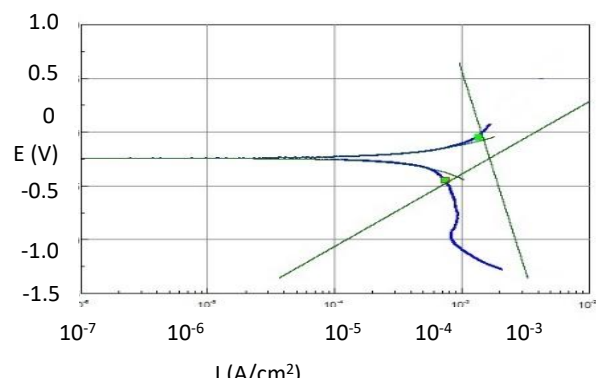
**Fig. 19** Tafel plot of OPC and SGPC under sulphate environment (4 g/l) at 180 days

317



Corrosion rate (mm/a) = 0.709

(a) Tafel plot of M1-OPC concrete sample exposed to  $\text{MgSO}_4$  (4 g/l) at 365 days



Corrosion rate (mm/a) = 0.664

(b) Tafel plot of M2-SGPC concrete sample exposed to  $\text{MgSO}_4$  (4 g/l) at 365 days

**Fig. 20** Tafel plot of OPC and SGPC at 365 days

318 Typical Tafel polarization curve fitting results for a passive and an active specimen are presented  
 319 in the above graphs for water cured and exposed samples ( $\text{MgSO}_4$ , 2 g/l or 4 g/l). The horizontal  
 320 axis is the logarithm of current density, and the vertical axis indicates electrical potential. Straight  
 321 lines are used to show the theoretical current for the anodic and cathodic reactions. The combined  
 322 anodic and cathodic current is shown by the curved lines. The extent of corrosion can be measure  
 323 from the distance between the intersection point and the curve line i.e. as we move away from the

324 curves corrosion rate increases and vice-versa. In the above graphs, it is evident that corrosion has  
325 occurred in both cases. The corrosion rate can be compared for the specimens cured in water or  
326 the sulphate solution. The corrosion rate of the specimens cured in sulphate was higher than the  
327 specimens cured in water. For example, when mixes of M1-OPC and M2-SGPC exposed to  
328  $MgSO_4$  (4 g/l) at 365 days are compared with water cured specimens at 365 days, it shows a  
329 corrosion rate of 0.709, 0.664 and 0.098, 0.087 respectively. This higher corrosion rate might be  
330 because of higher permeability as confirmed by RCPT and sorptivity test results above. Also, the  
331 N-A-S-H and C-A-S-H formation were less in SGPC when exposed to  $MgSO_4$  (4 g/l), as confirmed  
332 by EDS results above. The above observations confirm that corrosion rate is in line with the  
333 compressive strength, RCPT and sorptivity test results. Further higher corrosion in the  $MgSO_4$   
334 solution cured specimens when compared with water might be because of reduced alkalinity and  
335 transformation of  $\gamma-Fe_2O_3$  layer converts into iron sulphate. When Sulphate salts come into contact  
336 with steel, they lead to the formation of iron sulphate, placing oxy-hydroxide film on the surface  
337 of rebar. This film of iron sulphate is less protective than original passive iron oxide film. Sulphate  
338 salt is also responsible for leaching and formation of complex and expansive salt reducing the  
339 alkalinity and because of this rate of corrosion increases (Somuah et al. 1991; Berrocal et al. 2016).

340 In addition, this result shows that SGPC performed better than OPC in terms of corrosion. From  
341 Tafel plots (Figs. 15 to 20), it is obvious that the rate of corrosion increased with the exposure time  
342 in  $MgSO_4$  solution. (Morla et al. 2021) also studied the corrosion evaluation GPC concrete and  
343 concluded that the GPC has a higher resistance to chloride-induced corrosion, with a low corrosion  
344 rate and lower mass loss percentage, compared to conventional concrete. The results concluded  
345 that GPC reduced the corrosion rate compared to OPC, and provided satisfactory results from a  
346 durability perspective.

#### 347 **4. Conclusions**

348 Based on the observations and the results presented above the following conclusions can be  
349 derived upon

- 350 • The slump and compaction factor of all the mixes were above 100 mm and 0.90, respectively,  
351 which shows good workability per Indian standards.

- 352 • The compressive strength of water cured samples increased with age and this observation  
353 was obtained for both the mixes. The highest compressive strength for M1-OPC and M2-  
354 SGPC was 43.65 and 50.78 MPa at the age of 365 days. The higher compressive strength of  
355 M2-SGPC was due to denser microstructure and formation of addition (C-A-S-H and N-A-  
356 S-H) gels. The presence of finer alcofines (UFS) also contributed to this strength  
357 enhancement.
- 358 • The strength of samples exposed to  $MgSO_4$  salts decreased. The maximum percentage loss  
359 of the compressive strength for M1-OPC and M2-SGPC mixes was 55.97% and 36.53%,  
360 respectively, when the specimens were exposed to  $MgSO_4$  (4 g/l).
- 361 • Microstructural studies show that the degradation in the compressive strength of M1-OPC  
362 and M2-SGPC under  $MgSO_4$  was caused by C-S-H and N-A-S-H gels interacting with salts,  
363 resulting in low strength with the decrease in formation of C-A-S-H and N-A-S-H.
- 364 • This study shows that reinforced SGPC had a lower corrosion rate than OPC even in  
365 aggressive suplahte environment.

366 All above observations and finding suggest that SGPC performed better than OPC in both normal  
367 and aggressive sulpahte environments.

## 368 5. Recommendation

369 From the above findings and observation, the following recommendations can be made for future  
370 studies as follows:

- 371 • By inclusion of alcofine (UFS) along with the main binder (GGBFS) in geopolymer  
372 concrete, a high strength can be achieved at ambient temperature.
- 373 • Conventional concrete is more prone to higher concentrations of  $MgSO_4$  salts than slag-  
374 based geopolymer concrete. Therefore, SGPC can be used to replace OPC concrete at harsh  
375 conditions.
- 376

## 377 6. Future scope

- 378 • Durability of GPC shall be checked for freezing and thawing, alkali-silica reaction and  
379 other acidic environments.
- 380 • This study reports the durability of conventional and geopolymer concrete produced using  
381 NaOH and Na<sub>2</sub>SiO<sub>3</sub> as an alkaline-activators. However, the durability properties of the  
382 geopolymer concrete can be examined by using different alkaline activators such as  
383 potassium hydroxide and sodium carbonate.
- 384 • Durability of geopolymer concrete which has been cured at a high temperature.

### 385 **Acknowledgement**

386 The authors are highly thankful to the administrative support provided by DCR University of  
387 Science and Technology, Murthal, Sonipat.

### 388 **Statements and declarations**

389 Ethical Approval, Consent to Participate and Consent to Publish: Not required or applicable.  
390 Authors Contributions:

391 Atul Garg: Conceptualization, Software, Data curation, Writing- Original draft preparation,  
392 Visualization, Investigation.

393 Parveen: Conceptualization, Software, Data curation, Writing- Original draft preparation,  
394 Visualization, Investigation, Reviewing and Editing.

395 Dharendra Singhal: Reviewing and Editing.

396 Thong M Pham: Reviewing and Editing.

397 Deepankar Kumar Ashish: Reviewing and Editing.

### 398 **Funding**

399 No funds, grants, or other support were received during the preparation of this manuscript.

### 400 **Competing Interests**

401 The authors have no relevant financial or non-financial interests to disclose.

402 **Data availability and materials**

403 Not applicable

404



405 **References**

406 Albitar M, Mohamed Ali M.S, Visintin P, Drechsler M (2017) Durability evaluation of  
407 geopolymer and conventional concretes. *Construction and Building Materials*, 136, 374–385.  
408 <https://doi.org/10.1016/j.conbuildmat.2017.01.056>.

409  
410 Aljerf L (2015) Effect of Thermal-cured Hydraulic Cement Admixtures on the mechanical  
411 properties of concrete. *Interceram. - Int. Ceram. Rev.* 64, 346–356.  
412 <https://doi.org/10.1007/BF03401142>

413  
414 Bakharev T (2005a) Durability of geopolymer materials in sodium and magnesium sulfate  
415 solutions. *Cement and Concrete Research*, 35(6), 1233–1246.  
416 <https://doi.org/10.1016/j.cemconres.2004.09.002>

417  
418 Bakharev T (2005b) Resistance of geopolymer materials to acid attack. *Cement and Concrete*  
419 *Research*, 35(4), 658–670. <https://doi.org/10.1016/j.cemconres.2004.06.005>

420  
421 Balamuralikrishnan R, Saravanan J (2021) Effect of addition of alcofine on the compressive  
422 strength of cement mortar cubes. *Emerging Science Journal*, 5(2), 155–170.  
423 <https://doi.org/10.28991/esj-2021-01265>

424  
425 Barcelo L, Kline J, Walenta G, Gartner E (2014) Cement and carbon emissions. *Materials and*  
426 *Structures/Materiaux et Constructions*, 47(6), 1055–1065. [https://doi.org/10.1617/s11527-013-](https://doi.org/10.1617/s11527-013-0114-5)  
427 [0114-5](https://doi.org/10.1617/s11527-013-0114-5)

428  
429 Berrocal, C. G., Lundgren, K., & Löfgren, I. (2016) Corrosion of steel bars embedded in fibre  
430 reinforced concrete under chloride attack: State of the art. *Cement and Concrete Research*, 80, 69–  
431 85. <https://doi.org/10.1016/j.cemconres.2015.10.006>

432  
433 Buenfeld NR, Newman JB (1984) The permeability of concrete in a marine environment.

434 Magazine of Concrete Research, 36(127), 67–80. <https://doi.org/10.1680/mac.1984.36.127.67>  
435  
436 IS 383 (2016) Coarse and Fine Aggregate for Concrete- Specification. In Bureau of Indian  
437 Standard, BIS, New Delhi India 110002.  
438  
439 Edser C (2005) Reducing the environmental impact of laundry. Focus on Surfactants, 2005(4), 1–  
440 2. [https://doi.org/10.1016/s1351-4210\(05\)70693-4](https://doi.org/10.1016/s1351-4210(05)70693-4)  
441  
442 Gupta N, Siddique R (2020) Durability characteristics of self-compacting concrete made with  
443 copper slag. Construction and Building Materials, 247.  
444 <https://doi.org/10.1016/j.conbuildmat.2020.118580>  
445  
446 Hendriks CA, Worrell E, Jager Dde, Blok K, Riemer P (2003) Emission Reduction of Greenhouse  
447 Gases from the Cement Industry. Greenhouse Gas Control Technologies Conference, 1–11.  
448 <https://doi.org/10.1016/B978-008043018-8/50150-8>  
449  
450 IS 10262 (2019) Concrete mix Proportioning – Guidelines (Second Revision) Bureau of Indian  
451 Standard, New Delhi India 110002.  
452  
453 IS 516 (2018) Indian Standard Methods of Tests for Strength of Concrete (First Revision) Bureau  
454 of Indian Standard, New Delhi India 110002.  
455  
456 Jindal BB, Singhal D, Sharma S, Parveen (2018) Enhancing mechanical and durability properties  
457 of geopolymer concrete with mineral admixture. Computers and Concrete, 21(3), 345–353.  
458 <https://doi.org/10.12989/cac.2018.21.3.345>  
459  
460 Joseph B, Mathew G (2012) Influence of aggregate content on the behavior of fly ash based  
461 geopolymer concrete. Scientia Iranica, 19(5), 1188–1194.

462 <https://doi.org/10.1016/j.scient.2012.07.006>

463

464 Liptak BG (1974) “Water pollution” V.1, Environmental Engineer’s Handbook, pp 1-419

465

466 Malhotra VM (2010) Global warming and role of supplementary cementing materials and  
467 superplasticisers in reducing greenhouse gas emissions from the manufacturing of portland  
468 cement. International Journal of Structural Engineering, 1(2), 116–130.

469 <https://doi.org/10.1504/ijstructe.2010.031480>

470

471 Mathew NS, Usha S (2016) Effects of Copper Slag as Partial Replacement for Fine Aggregate in  
472 Geopolymer Concrete. In IOSR Journal of Mechanical and Civil Engineering, 73-77

473

474 Morla P, Gupta R, Azarsa P, Sharma A (2021) Corrosion evaluation of geopolymer concrete made  
475 with fly ash and bottom ash. Sustainability (Switzerland), 13(1), 1–16.

476 <https://doi.org/10.3390/su13010398>

477

478 Muhammed N, Shihab L, Sakin S (2022) Ultimate Load of Different Types of Reinforced Self-  
479 Compacting Concrete Columns Attacked by Sulphate. Civil Engineering Journal (Iran), 8(10),  
480 2069–2083. <https://doi.org/10.28991/CEJ-2022-08-10-04>

481

482 Mustakim SM, Das SK, Mishra J, Aftab A, Alomayri TS, Assaedi HS, Kaze CR (2021)  
483 Improvement in Fresh, Mechanical and Microstructural Properties of Fly Ash- Blast Furnace Slag  
484 Based Geopolymer Concrete By Addition of Nano and Micro Silica. Silicon, 13(8), 2415–2428.

485 <https://doi.org/10.1007/s12633-020-00593-0>

486

487 Parveen, Mehta A, Saloni (2019) Effect of ultra-fine slag on mechanical and permeability  
488 properties of Metakaolin-based sustainable geopolymer concrete. Advances in Concrete  
489 Construction, 7(4), 231–239. <https://doi.org/10.12989/acc.2019.7.4.231>

490

491 Parveen, & Singhal D (2017) Development of mix design method for geopolymer concrete.

492 Advances in Concrete Construction, 5(4), 377–390. <https://doi.org/10.12989/acc.2017.5.4.377>  
493

494 Parveen, Singhal D, Junaid MT, Jindal BB, Mehta A (2018) Mechanical and microstructural  
495 properties of fly ash based geopolymer concrete incorporating alcofine at ambient curing.  
496 Construction and Building Materials, 180(2018), 298–307.  
497 <https://doi.org/10.1016/j.conbuildmat.2018.05.286>  
498

499 Pasupathy K, Sanjayan J, Rajeev P, Law DW (2021) The effect of chloride ingress in reinforced  
500 geopolymer concrete exposed in the marine environment. Journal of Building Engineering,  
501 39(February), 102281. <https://doi.org/10.1016/j.jobbe.2021.102281>  
502

503 Patankar SV, Jamkar SS, Ghugal YM (2013) Effect of Water-To-Geopolymer Binder Ratio on the  
504 Production of Fly Ash Based Geopolymer Concrete. International Journal of Advanced  
505 Technology in Civil Engineering, 1, 79–83. <https://doi.org/10.13140/2.1.4792.1284>  
506

507 IS 4563 (2000) Plain and Reinforced Concrete - Code of Practice. Bureau of Indian Standard,  
508 New Delhi India 110002.  
509

510 Punurai W, Kroehong W, Saptamongkol A, Chindaprasirt P (2018) Mechanical properties,  
511 microstructure and drying shrinkage of hybrid fly ash-basalt fiber geopolymer paste. Construction  
512 and Building Materials, 186, 62–70. <https://doi.org/10.1016/j.conbuildmat.2018.07.115>  
513

514 Robayo-Salazar R, Mejia-Arcila J, Mejia de Gutierrez R, Martinez E (2018) Life cycle assessment  
515 (LCA) of an alkali-activated binary concrete based on natural volcanic pozzolan: A comparative  
516 analysis to OPC concrete. Construction and Building Materials, 176, 103–111.  
517 <https://doi.org/10.1016/j.conbuildmat.2018.05.017>  
518

519 Saloni, Parveen, Pham TM, Lim YY, Pradhan SS, Jatin, Kumar J (2021) Performance of rice husk  
520 Ash-Based sustainable geopolymer concrete with Ultra-Fine slag and Corn cob ash. Construction  
521 and Building Materials, 279, 122526. <https://doi.org/10.1016/j.conbuildmat.2021.122526>

522

523 Saloni, Singh A, Sandhu V, Jatin, Parveen (2020) Effects of alcofine and curing conditions on  
524 properties of low calcium fly ash-based geopolymer concrete. *Materials Today: Proceedings*.  
525 <https://doi.org/10.1016/j.matpr.2020.02.763>

526

527 Sangoju B, Bharatkumar BH, Gettu R, Srinivasan P, Ramanjaneyulu K, Iyer NR (2015) Influence  
528 of PCE-SP and calcium nitrite inhibitor on mechanical and durability parameters of concrete.  
529 *Journal of Scientific and Industrial Research*, 74(2), 82–87.

530

531 Sasui S, Kim G, Nam J, Koyama T, Chansomsak S (2020) Strength and microstructure of class-C  
532 fly ash and GGBS blend geopolymer activated in NaOH & NaOH + Na<sub>2</sub>SiO<sub>3</sub>. *Materials*, 13(1).  
533 <https://doi.org/10.3390/ma13010059>

534

535 Somuah SK, Boah JK, Leblanc P, Al-Tayyib AJ, Al-Mana AI (1991) Effect of Sulfate and  
536 carbonate ions on reinforcing steel corrosion as evaluated using AC impedance spectroscopy. *ACI*  
537 *Material JL*, 88, PP 49-55. <https://doi.org/10.14359/2364>

538

539 Souza DJde, Medeiros MHFde, Hoppe Filho J (2020) Evaluation of external sulfate attack  
540 (Na<sub>2</sub>SO<sub>4</sub> and MgSO<sub>4</sub>): Portland cement mortars containing siliceous supplementary cementitious  
541 materials. *Revista IBRACON de Estruturas e Materiais*, 13(4), 1–16.  
542 <https://doi.org/10.1590/s1983-41952020000400003>

543

544 Thanh TP, Nguyen TT, Nguyen TT (2022) Experimental Evaluation of Geopolymer Concrete  
545 Strength Using Sea Sand and Sea Water in Mixture. *Civil Engineering Journal (Iran)*, 8(8), 1574–  
546 1583. <https://doi.org/10.28991/CEJ-2022-08-08-03>.

547

548 Vázquez-Rowe I, Ziegler-Rodriguez K, Laso J, Quispe I, Aldaco R, Kahhat R (2019) Production  
549 of cement in Peru: Understanding carbon-related environmental impacts and their policy  
550 implications. *Resources, Conservation and Recycling*, 142(December), 283–292.

551 <https://doi.org/10.1016/j.resconrec.2018.12.017>

552

553 Wee TH, Suryavanshi AK, Tin SS (2000) Evaluation of rapid chloride permeability test (RCPT)  
554 results for concrete containing mineral admixtures. *Ac Structural Journal* 97(2):221-232,  
555 97(2), 21–232.